Talanta 127 (2014) 163–168

Contents lists available at ScienceDirect

Talanta

journal homepage: www.elsevier.com/locate/talanta

A sensitive gold nanoparticle-based colorimetric aptasensor for *Staphylococcus aureus*

Jinglei Yuan, Shijia Wu, Nuo Duan, Xiaoyuan Ma, Yu Xia, Jie Chen, Zhansheng Ding, Zhouping Wang*

State Key Laboratory of Food Science and Technology, Synergetic Innovation Center of Food Safety and Nutrition, School of Food Science and Technology, Jiangnan University, Wuxi 214122, China

ARTICLE INFO

Article history:
Received 10 February 2014
Received in revised form
29 March 2014
Accepted 4 April 2014
Available online 13 April 2014

Keywords:
Staphylococcus aureus
Tyramine signal amplification
Aptamer
Gold nanoparticles

ABSTRACT

In this study, a gold nanoparticle-based colorimetric aptasensor for *Staphylococcus aureus* (*S. aureus*) using tyramine signal amplification (TSA) technology has been developed. First, the biotinylated aptamer specific for *S. aureus* was immobilized on the surface of the wells of the microtiter plate via biotin–avidin binding. Then, the target bacteria (*S. aureus*), biotinylated-aptamer–streptavidin-HRP conjugates, biotinylated tyramine, hydrogen peroxide and avidin–catalase were successively introduced into the wells of the microtiter plate. After that, the existing catalase consumed the hydrogen peroxide. Finally, the freshly prepared gold (III) chloride trihydrate was added, the color of the reaction production would be changed and the absorbance at 550 nm could be measured with a plate reader. Under optimized conditions, there was a linear relationship between the absorbance at 550 nm and the concentration of *S. aureus* over the range from 10 to 10^6 cfu mL^{-1} (with an R^2 of 0.9947). The limit of the developed method was determined to be 9 cfu mL^{-1}.

1. Introduction

Staphylococcus aureus (*S. aureus*) is an important bacterial pathogen that produces a variety of toxins and causes a wide range of infections, including soft-tissue infection, Staphylococcal food poisoning, and even life-threatening diseases [1], such as pneumonia, endocarditis, osteomyelitis, arthritis, and sepsis. *S. aureus* is one of the top five pathogens that contribute to foodborne illnesses in America [2]. Therefore, it is of great importance to develop a simple, specific, and sensitive detection method for *S. aureus*.

To date, several commonly used methods for the detection of *S. aureus* have been developed, including colony counting, enzyme-linked immunosorbent assay (ELISA) [3], the polymerase chain reaction (PCR) technique [4], and loop-mediated isothermal amplification (LAMP) [5]. These methods have been successfully applied in various fields. However, some of the methods have deficiencies in stability, price, accuracy, detection limits or time. The development of a novel detection method with the advantages of simplicity, speed and sensitivity has been attracting increased attention. In addition, some colorimetric assays for the detection of *S. aureus* have been developed [6]. However, the aptamers have not been used in the colorimetric assays for *S. aureus* before.

Aptamers are DNA or RNA molecules that are commonly obtained *in vitro* using a combinatorial chemistry technique known as systematic evolution of ligands by exponential enrichment (SELEX) [7]; and some aptamers of targets were already obtained using the SELEX technique, such as *Salmonella enterica* [8], *Streptococcus pyogenes* [9], *Escherichia coli* [10], zearalenone [11], *S. aureus* enterotoxin A [12] and B [13], bisphenol A [14], and cancerous cells [15]. Compared with antibodies, aptamers are easy to obtain and are more stable towards biodegradation. Moreover, because of the ability of aptamers to bind to their target molecules with high affinity and specificity, aptamers have been widely used as a useful tool for the detection of certain pathogenic bacteria [16,17], toxins [18–21], heavy metal ions [22,23], proteins [24], illegal food additives [25] and even cancerous cells [26].

Colorimetric detection methods are convenient and effective in many applications because the readout requires only human eyes [27]. Gold nanoparticles (AuNPs) possess the unique characteristic of the well-dispersed AuNP solution being red and the aggregated AuNP solution being blue or purple; therefore, AuNP-based colorimetric assays have been used recently for the detection of various substances, including amino acids [28], toxins [29], DNA [30,31], heavy metal ions [32], illegal food additives [33,34], pesticide residues [35], disease biomarkers [36] and cancerous cells [37]. Additionally, a major advantage of this colorimetric assay is that

* Corresponding author. Tel./fax: +86 510 8532 6195.
E-mail address: wangzp@jiangnan.edu.cn (Z. Wang).

http://dx.doi.org/10.1016/j.talanta.2014.04.013
0039-9140/

the analyte can be easily detected using the naked eye, and no sophisticated instruments are required.

In the present work, a novel gold nanoparticle-based colorimetric assay for *S. aureus* using aptamer recognition and tyramine signal amplification (TSA) technology has been developed. The biotinylated aptamer can bind to *S. aureus* with high affinity and specificity, and the *S. aureus* can be captured and fixed on the bottom of the microtiter plates through the specific binding between biotin and avidin. Then, a large amount of the catalase can bind to the surface of the *S. aureus* with the help of the tyramine signal amplification technology, and the enzyme catalase can consume H_2O_2. This reaction slows down the kinetics of crystal growth, and aggregated nanoparticles are formed, which causes the solution to turn blue. In the absence of the target (*S. aureus*), the concentration of H_2O_2 was high, and the reduction of gold ions via H_2O_2 occurs at a rapid rate, which forms non-aggregated and spherical nanoparticles, and the solution is red. Compared to the existing methods, such as the microbiological culture method, ELISA and PCR, the developed method offers the merits of simplicity, rapidity, sensitivity, stability and low cost. This work increases the scope of TSA technology coupled with aptamer applications.

2. Materials and methods

2.1. Reagents and apparatus

Anhydrous sodium carbonate (Na_2CO_3), sodium bicarbonate ($NaHCO_3$), 30% hydrogen peroxide (30% H_2O_2), gold (III) chloride trihydrate ($HAuCl_4$), dimethyl sulfoxide (DMSO), sodium chloride (NaCl), tris (hydroxymethyl) aminomethane, potassium chloride (KCl), disodium hydrogen phosphate ($Na_2HPO_4 \cdot 12H_2O$), dipotassium hydrogen phosphate (K_2HPO_4), agar powder, tryptone, yeast extract, N,N-dimethylformamide (DMF), ethanol, triethylamine, Tween-20, and bovine serum albumin (BSA) were purchased from the Sinopharm Chemical Reagent Co., Ltd. (Shanghai, China). Streptavidin-horseradish peroxidase (Streptavidin-HRP) and N-hydroxysuccinimide biotin (NHS Bioth) were purchased from the Shanghai Sangon Biological Science & Technology Company (Shanghai, China). Catalase and avidin were purchased from Sigma–Aldrich. SM(PEG)24 was purchased from Thermo Scientific. Tyramine hydrochloride was purchased from the Shanghai yuanye Bio-Technology Co., Ltd. (Shanghai, China). MES was purchased from the Aladdin industrial Corporation (Shanghai, China). *S. aureus* ATCC 29213 was obtained from the American Type Culture Collection (ATCC). The *S. aureus* aptamer [38] 5'-biotin-C6-GCA ATG GTA CGG TAC TTC CTC GGC ACG TTC TCA GTA GCG CTC GCT GGT CAT CCC ACA GCT ACG TCA AAA GTG CAC GCT ACT TTG CTA A-3' was synthesized by the Shanghai Sangon Biological Science & Technology Company (Shanghai, China). The signals were scanned using a Molecular Devices SpectraMax M5 plate reader (M5, Molecular Devices, U.S.A.), and the milk sample was centrifuged using a Centrifuge 5430R (5430R, Eppendorf, Germany). The ultrapure water used in the experiments was prepared using a Millipore Direct-Q® 3 system (Merck Millipore, MA, U.S.A.) and had a resistivity of 18.2 MΩ cm.

2.2. Preparation of biotin–tyramine

The biotin–tyramine conjugate was prepared according to the Hopman's method [39]: 10 mg Bio-NHS was dissolved in 1 mL of DMF to prepare solution A; 2.8 mg of tyramine hydrochloride was dissolved in 0.28 mL of DMF, and 2.8 μL of triethylamine was added into solution A to prepare solution B; then, solution A and solution B were mixed and reacted in the dark at room temperature for 2 h. Finally, 8.72 mL ethanol was added to prepare a 10 mL biotin–tyramine stock solution, which was stored at 4 °C in the dark.

2.3. Preparation of avidin–catalase

The process of the avidin–catalase conjugation was as follows: 4 μL of SM(PEG)24 (250 mmol L^{-1} in dry DMSO) and 1 mL of avidin (1 mg mL^{-1}) were mixed, and the reaction was incubated for 30 min at room temperature. The excess cross-linker was removed with a dialysis bag. Then, 5 mg of catalase was added, and the reaction mixture was incubated at room temperature for 30 min. Finally, the avidin–catalase conjugation was stored at 4 °C until used.

2.4. Assembly of aptamer onto the microtiter plate wells

First, the avidin (1 mg mL^{-1}) was diluted 1:100 with carbonate buffer (pH 9.6), and 200 μL of diluted avidin was added into each well of the microtiter plates and incubated at 4 °C overnight. After washing with the wash buffer (0.01 mol L^{-1} PBS, 0.05% Tween-20) 3 times (1 min per wash), each well in the microtiter plates was blocked with a blocking buffer (1 mg mL^{-1} BSA in 0.01 mol L^{-1} PBS) for 1 h at room temperature to prevent the appearance of false positive signals. Subsequently, the microtiter plates were washed 3 times with the wash buffer, and 10 μL of biotinylated aptamer was added and incubated at 37 °C. After 30 min, the microtiter plates were washed 3 times with the wash buffer, and air dried.

2.5. Analytical procedure

A 100 μL aliquot of a sample solution containing *S. aureus* was added to each well of the microtiter plates. The biotinylated aptamer and streptavidin-HRP were mixed and then incubated at 37 °C for 30 min at the same time. The microtiter plates were washed 3 times with wash buffer, and 10 μL samples of the aptamer and streptavidin-HRP complexes were added to the microtiter plates and incubated at 37 °C for 30 min. After washing 3 times with the wash buffer, each well of the microtiter plates was loaded with 10 μL of biotin–tyramine. A small volume of hydrogen peroxide (0.5%, v/v) [40] was also added to the diluted solution to act as the oxidizing agent of tyramine. The microtiter plates were incubated at 37 °C for 30 min and then washed 3 times with the wash buffer and air dried. Subsequently, 100 μL of avidin–catalase was added into each well of the microtiter plates. The plates were incubated at 37 °C for 30 min and then washed 5 times with the wash buffer, once with deionized water, and air dried. Then, 100 μL of 280 μmol L^{-1} H_2O_2 in MES buffer (1 mmol L^{-1}, pH 6.5) was added, and the microtiter plates were incubated at room temperature for 30 min. Finally, 100 μL of freshly prepared gold (III) chloride trihydrate (0.2 mmol L^{-1}) in MES buffer was added to each well. After 15 min, the absorbance at 550 nm was recorded using a Molecular Devices SpectraMax M5 plate reader. This procedure is illustrated in Fig. 1, and the color is formed by the reaction in the microtiter plate.

2.6. Treatment of the milk samples

Raw milk was purchased from local supermarkets. First, a 10 mL milk sample was centrifuged for at least 15 min at 12,000 rpm to eliminate protein and fat. Second, the obtained supernatant was filtered with a 0.22 μm filtration membrane twice and then adjusted to pH 7.7 using Tris-HCl buffer. Third, the milk sample was divided into nine sections, and the volume of each was

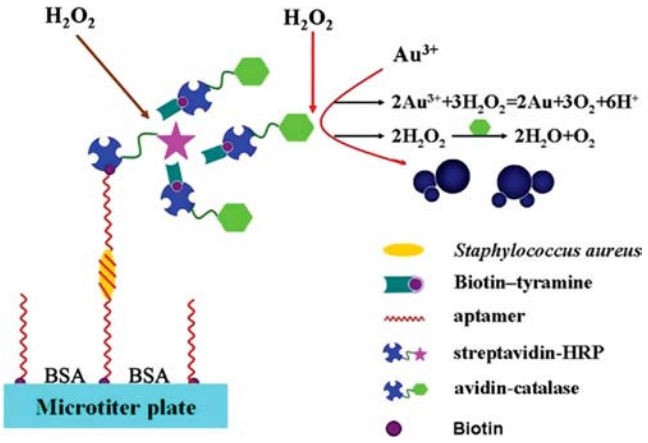

Fig. 1. Schematic illustration of the colorimetric and visual detection of *Staphylococcus aureus* based on tyramine signal amplification coupled with aptamer recognition.

900 μL. Finally, 100 μL of different concentrations of *S. aureus* were added to the treated milk samples to make the spiked samples.

3. Results and discussion

3.1. Optimization of the concentration of the aptamer

The microtiter plate was covered with avidin, and the biotinylated aptamer was fixed on the bottom of the microtiter plate through the specific binding between biotin and avidin. The role of the aptamer was to capture *S. aureus* and attach it to the bottom of the microtiter plates; therefore, the concentration of the aptamer directly influenced the amount of the captured *S. aureus* and the intensity of the signals. To obtain the optimized concentration of aptamer, different concentrations ranging from 10^{-5} to 10^{-12} mol L^{-1} were used to detect the same sample (10^6 cfu mL^{-1}) And the concentrations of *S. aureus* were determined by the classical counting methods. As shown in Fig. 2a, the intensity of the signals decreased as the concentration of the aptamer decreased over the concentration range of 10^{-12} mol L^{-1}–10^{-6} mol L^{-1}, and the absorbance at 550 nm obtained became lower as the concentration of the captured *S. aureus* increased. However, for the concentrations of 10^{-6} and 10^{-5} mol L^{-1}, there was only a slight difference between the intensities of the signals. Consequently, the 10^{-6} mol L^{-1} was detected as the optimized concentration of aptamer.

3.2. Optimization of the dilution of streptavidin-HRP

In this work, the role of the streptavidin-HRP was mainly to catalyze the tyramine deposition, and the signal intensity was minimally affected by the concentration of streptavidin-HRP [40]. A series of streptavidin-HRP (1 mg mL^{-1}) dilution of 1:500, 1:1500, 1:3000, 1:4500, and 1:6000 were set and used for the detection of the sample (the concentration of *S. aureus* in the sample was 10^6 cfu mL^{-1}). The result indicated that the concentration of the streptavidin-HRP had a limited influence on the signal intensities of the samples, and the ideal dilution ratio of the streptavidin-HRP was defined as 1:1500 in this work.

3.3. Optimization of the dilution of biotin–tyramine

Tyramine is a phenolic compound, and HRP can catalyze biotin–tyramine to produce highly reactive phenolic radicals (tyramide radicals) in the presence of H_2O_2, which react covalently with the electron-rich moieties of protein molecules that are present in the vicinity of the HRP label. Fig. 2b indicates that the intensity of the signals gradually declines as the biotin–tyramine dilution ratio increases from 1:50 to 1:100, and the intensity becomes stronger sharply as the biotin–tyramine dilution ratio increases from 1:100 to 1:800. This trend may occur because HRP

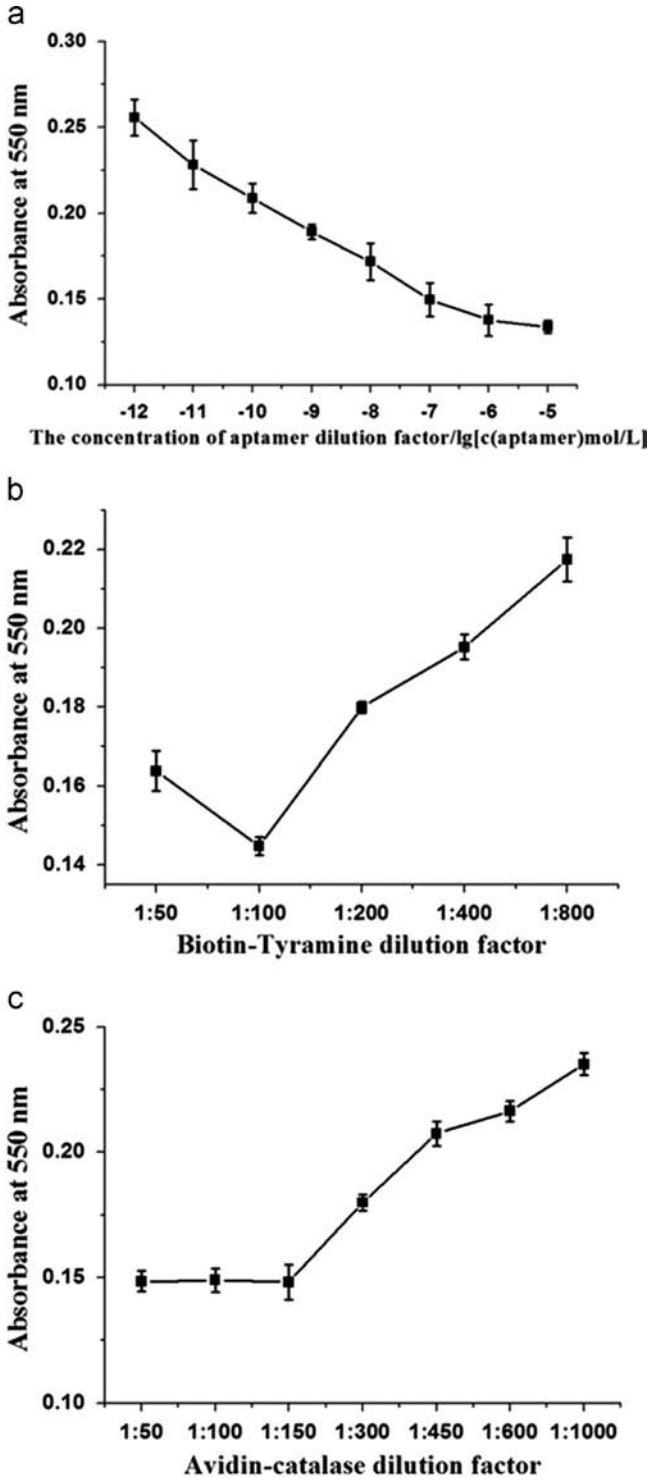

Fig. 2. Optimization of the experiment conditions. (a) Optimization of the concentration of aptamer, and the concentration of aptamer was from 10^{-5} to 10^{-12} mol L^{-1}. (b) Plot used to optimize the dilutions of biotin–tyramine, and a series of biotin–tyramine dilutions of 1:50, 1:100, 1:200, 1:400, and 1:800 were set in blocking buffer (1 mg mL^{-1} BSA in 0.01 mol L^{-1} PBS). (c) Effect of the dilution of avidin–catalase on the signal intensity, and the avidin–catalase was diluted with the dilution ratio from 1:50 to 1:1000 in blocking buffer. The concentration of *S. aureus* in the sample detected was 10^6 cfu mL^{-1}.

can catalyze the dimerization of tyramine when it is present at a high concentration, which is likely caused by the generation of free radicals [41]. However, when the tyramine is applied in lower concentrations, the probability of dimerization is reduced because the binding of highly reactive intermediates to electron-rich moieties of proteins is favored [42]. The number of highly reactive intermediates that are generated by HRP catalysis was low when the concentration of tyramine was also low. Therefore, the 1:100 dilution was suitable for the experiment.

3.4. Optimization of the dilution of avidin–catalase

In this work, the enzyme catalase can consume H_2O_2, which has a great influence on the intensity of the signal. The avidin–catalase was diluted to 1:50, 1:100, 1:150, 1:300, 1:450, 1:600, and 1:1000 with the blocking buffer for the detection of the same sample (the concentration of *S. aureus* in the sample was 10^6 cfu mL^{-1}). As shown in Fig. 2c, the signal intensity becomes stronger and stronger as the avidin–catalase dilution ratio increases from 1:150 to 1:1000, and the signal intensity increases minimally as the avidin–catalase dilution ratio increases from 1:50 to 1:150. In other words, for dilutions of 1:50, 1:100 and 1:150, there was a slight difference between the intensities of the signals that correlated with the dilution of avidin–catalase. When the dilution ratio was between 1:50 and 1:150, the concentration of avidin–catalase was sufficient for this work, and the intensity of the signals would not increase as the avidin–catalase dilution ratio increases from 1:50 to 1:150. Thus, 1:150 was detected as the optimized dilution of avidin–catalase in this experiment.

3.5. Specificity

To evaluate the specificity of this method, six other samples containing *Vibrio parahemolyticus*, *Salmonella typhimurium*, *Streptococcus*, *Enterobacter sakazakii*, *E. coli* and *Listeria monocytogenes* and one blank sample were measured. The analysis of all samples was performed under the same conditions, and the concentrations of all bacteria were from 10 to 10^7 cfu mL^{-1}. Fig. 3A clearly shows that the intensity of the signals of the other six bacteria and the blank sample would not change as the concentrations of all bacteria increased, and the intensity of the signals was much higher than the *S. aureus* samples. In addition, 10^6 cfu mL^{-1} was selected as the representative concentrations for all bacteria. In Fig. 3B, the color of *S. aureus* was blue, while the color of the other six bacterial samples and the blank sample was red. This result (Fig. 3) provides an absolute guarantee of the specific detection of *S. aureus*.

3.6. Analytical performance

A series of concentrations of *S. aureus* and some blank samples were investigated under optimal conditions. There was a strong linear correlation between the intensity of the signal and the concentration of *S. aureus* over the range from 10 to 10^6 cfu mL^{-1} (Fig. 4). The linear fit obtained gave $y=-0.0283x+0.3101$ ($R^2=0.9947$). The detection limit of the developed method was calculated based on $3<\sum>$/slope, where $<\sum>$ was the standard deviation of blank samples and slope was obtained from the standard correlation curve between the intensity of the signals and the concentration of *S. aureus*. The statistical analysis revealed that the detection limit of *S. aureus* was 9 cfu mL^{-1}.

Meanwhile, a series of concentrations of *S. aureus* were analyzed using the method without the tyramide signal amplification (TSA) technology. The linear correlation between the intensity of the signals and the concentration of *S. aureus* was 0.9940, but the linear range from 10^2 to 10^5 cfu mL^{-1} was very narrow, and the limit of detection was 85 cfu mL^{-1}. By considering the results from the comparison of these two methods, it was proved that the linear correlations, the linear range and the limit of detection were improved significantly by the TSA technology.

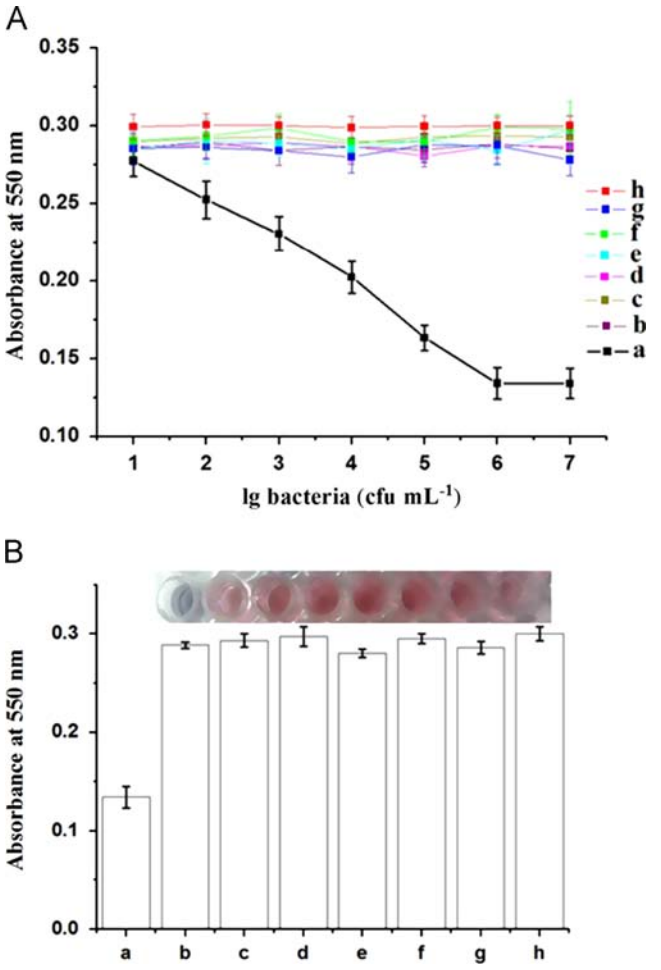

Fig. 3. The intensity of the signals measured for (a) *S. aureus*, (b) *Vibrio parahemolyticus*, (c) *Streptococcus*, (d) *Salmonella typhimurium*, (e) *E. sakazakii*, (f) *E. coli*, (g) *Listeria monocytogenes* and (h) the control. (A) Concentrations of all bacteria were from 10 to 10^7 cfu mL^{-1}, and (B) Concentrations of all bacteria were 10^6 cfu mL^{-1} (For interpretation of the reference to color in this figure, the reader is referred to the web version of this article.)

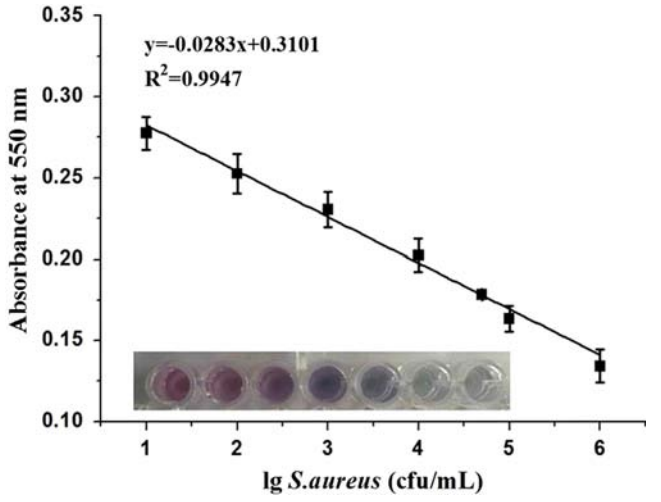

Fig. 4. Standard correlation curve between the intensity of the signals and the concentration of *S. aureus*.

Table 1
Figures of merits of comparable methods for determination of *Staphylococcus aureus*.

Method used	LOD (cfu mL^{-1})	Application	Analysis time (h)	Ref.
The sensitive fluorescent detection method using nanogold linked CdTe nanocrystals	50	Spiked milk samples	N.I.	[43]
Electrochemical immunosensor using 3,3-dithiodipropionic acid (N-succinimidyl ester)-modified gold electrodes	3.7×10^2	Semi-skimmed milk samples	2	[44]
Gold based immunosensors	10^5	N.I.	N.I.	[45]
The fluorescence detection method by using water-soluble CdSe quantum dots	10^2	N.I	1–2	[46]
Label-free detection method using real-time potentiometric biosensors based on carbon nanotubes and aptamers	8×10^2	Freshly excised dorsal pig skin	>1	[47]
The gold nanoparticle-based colorimetric aptasensor	9	Milk samples	<4	This work

N.I. –No information.

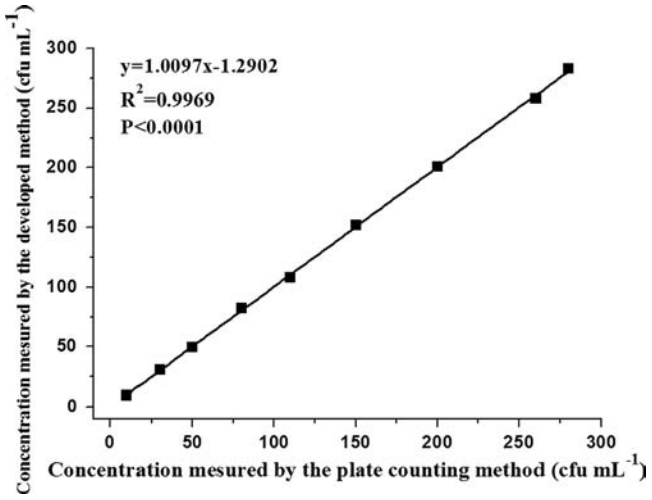

Fig. 5. Relationship between the proposed method and plate counting method for *S. aureus* detection in milk samples.

The developed method was further compared with some previous methods about the detection of *S. aureus* (Table 1). As shown in Table 1, the developed method is more sensitive and the detection limit was lower than others. However, the analysis time of the developed method should be improved and it would be taken into account in the future studies.

3.7. Method validation and calculate linear regression errors

Using the method developed here, 100 μL of the treated milk samples were tested, and an additional 100 μL samples were tested using the classical plate counting method. The analytical results are presented in Fig. 5.

The results obtained using the visual detection method were similar to the results obtained from the plate counting method. There was no significant difference between the counting method and the developed method ($R^2=0.9969$, $P<0.0001$), and the linear fit that was obtained was $y=1.0097x-1.2902$, which confirms that the colorimetric and visual detection method using aptamers coupled with TSA can be used for the detection of real samples.

4. Conclusion

In summary, a gold nanoparticle-based colorimetric assay for *S. aureus* using the recognition of aptamers coupled with TSA has been developed. The detection sensitivity of the developed method can reach 9 cfu mL^{-1}, and the linear range was wide (from 10 to 10^6 cfu mL^{-1}). In addition, this developed method was successfully used to analyze milk samples, and there was no significant difference between a classical plate counting method and the developed method. The detection method developed here could potentially be adapted for the detection of any analyte as long as the aptamers directed against were available. Therefore, the developed method has the potential for wide use in the visual detection of other foodborne pathogenic bacteria in food samples.

Acknowledgments

This work was partly supported by NSFC (21375049), National S&T Support Program of China (2012BAK08B01, 2011YQ170067), S&T Supporting Project of Jiangsu Province (BE2011621, BE2012614), JSCIQ_2012IK166, Research Fund for the Doctoral Program of Higher Education (20110093110002), NCET-11-0663, JUSRP51309A and JUSRP21125.

References

[1] P. Francois, A. Scherl, D. Hochstrasserb, J. Schrenzel, J. Proteomics 73 (2010) 701–708.
[2] S.P. Chakraborty, S.K. Mahapatra, S.K. Sahu, S. Chattopadhyay, P. Pramanik, S. Roy, Asian Pac. J. Trop. Biomed. 1 (2011) 102–109.
[3] J.M. Jay, M.J. Loessner, D.A. Golden, Modern Food Microbiology, Springer, New York, 2005.
[4] A. Huletsky, R. Girous, V. Rossbach, M. Gaqnon, M. Vaillancourt, M. Bernier, F. Gaqnon, K. Truchon, M. Bastien, F.J. Picard, A. Van Belkum, M. Ouellette, P. H. Roy, M.G. Berqeron, J. Clin. Microbiol. 42 (2004) 1875–1884.
[5] K.T. Lim, C.S. Teh, K.L. Thong, Biomed. Res. Int.2013 (2013) 895816.
[6] Y.J. Sung, H.Y. Suk, H.Y. Sung, T. Li, H. Poo, M.G. Kim, Biosens. Bioelectron. 43 (2013) 432–439.
[7] C.L.A. Hamula, J.W. Guthrie, H.Q. Zhang, X.F. Li, X.C. Le, Trends Anal. Chem. 25 (2006) 681–691.
[8] R. Joshi, H. Janagama, H.P. Dwivedi, T.M.A. Senthi Kumar, L.A. Jaykus, J. Schefers, S. Sreevatsan, Mol. Cell Probes 23 (2009) 20–28.
[9] C.L. Humula, X.C. Le, X.F. Li, Anal. Chem. 83 (2011) 3640–3647.
[10] J.G. Bruno, M.P. Carrillo, T. Phillips, C.J. Andrews, J. Fluoresc. 20 (2010) 1211–1223.
[11] X.J. Chen, Y.K. Huang, N. Duan, S.J. Wu, X.Y. Ma, Y. Xia, C.Q. Zhu, Y. Jiang, Z. P. Wang, Anal. Bioanal. Chem. 405 (2013) 6573–6581.
[12] Y.K. Huang, X.J. Chen, Y. Xia, S.J. Wu, N. Duan, X.Y. Ma, Z.P. Wang, Anal. Methods 6 (2014) 690–697.
[13] M. Jo, J.Y. Ahn, J. Lee, S. Lee, S.W. Hong, J.W. Yoo, J. Kang, P. Dua, D.K. Lee, S. Hong, S. Kim, Oligonucleotides 21 (2011) 85–91.
[14] J.A. DeGrasse, PLoS One 7 (2012) e33410.
[15] Z. Tang, D.H. Shangguan, K.H. Wang, K. Shi, K. Sefah, P. Mallikratchy, H. W. Chen, Y. Li, W. Tan, Anal. Chem. 79 (2007) 4900–4907.
[16] J.L. Yuan, Z. Tao, Y. Yu, X.Y. Ma, Y. Xia, L. Wang, Z.P. Wang, Food Control 37 (2014) 188–192.
[17] J.L. Yuan, Y. Yu, Can Li, X.Y. Ma, Y. Xia, J. Chen, Z.P. Wang, Microchim. Acta 181 (2014) 321–327.
[18] A. Hayat, A. Sassolas, J.L. Marty, A.E. Radi, Talanta 103 (2013) 14–19.
[19] M.L. Yang, B.Y. Jiang, J.Q. Xie, Y. Xiang, R. Yuan, Y.Q. Chai, Talanta 125 (2014) 45–50.
[20] C. Yang, V. Lates, B. Prieto-Simon, J.L. Marty, X. Yang, Talanta 116 (2013) 520–526.
[21] Z.P. Wang, N. Duan, X. Hun, S.J. Wu, Anal. Bioanal. Chem. 398 (2010) 2125–2132.

[22] Z.L. Jiang, G.Q. Wen, Y.Y. Fan, C. Jiang, Q.Y. Liu, Z. Huang, A.H. Liang, Talanta 80 (2013) 1287–1291.
[23] Y.W. Lin, C.W. Liu, H.T. Chang, Talanta 84 (2013) 324–329.
[24] J.A. Hansen, J. Wang, A.N. Kawde, Y. Xiang, K.V. Gothelf, G. Collins, J. Am. Chem. Soc. 128 (2006) 2228–2229.
[25] F. Xue, J.J. Wu, Y.Q. Chu, Z.L. Mei, Y.K. Ye, J. Liu, R. Zhang, C.F. Peng, L. Zheng, W. Chen, Microchim. Acta 180 (2013) 109–115.
[26] J.J. Li, M. Xu, H.P. Huang, J.J. Zhou, E.S. Abdel-Halimb, J.R. Zhang, J.J. Zhu, Talanta 85 (2011) 2113–2120.
[27] W.S. Qu, Y.,Y. Liu, D.B. Liu, Z. Wang, X.Y. Jiang, Angew. Chem. 123 (2011) 3504–3507.
[28] W.D. Pu, H.W. Zhao, C.Z. Huang, L.P. Wu, D. Xu, Anal. Chim. Acta 764 (2013) 78–83.
[29] C. Yang, Y. Wang, J.L. Marty, X.R. Wang, Biosens. Bioelectron. 26 (2011) 2724–2727.
[30] E. Liandris, M. Gazouli, M. Andreadou, M. Comor, N. Abazovic, L.A. Sechi, J. Ikonomopoulos, J. Microbiol. Methods 78 (2009) 260–264.
[31] J.H. Kim, B.H. Chung, Biosens. Bioelectron. 26 (2011) 2805–2809.
[32] J.S. Lee, M.S. Han, C.A. Mirkin, Angew. Chem. Int. Ed. 46 (2007) 4093–4096.
[33] Z.L. Mei, H.Q. Chu, W. Chen, F. Xue, J. Liu, H.N. Xu, R. Zhang, L. Zheng, Biosens. Bioelectron. 39 (2013) 26–30.
[34] H. Huang, L. Li, G.H. Zhou, Z.H. Liu, Q. Ma, Y.F. Feng, G.P. Zeng, P. Tinnefeld, Z. K. He, Talanta 85 (2011) 1013–1019.
[35] J.M. Zheng, H.J. Zhang, J.C. Qu, Q. Zhu, X.G. Chen, Anal. Methods 5 (2013) 917–924.
[36] R. de la Rica, M.M. Stevens, Nat. Nanotechnol. 7 (2012) 824.
[37] W.T. Lu, S.R. Arumugam, D. Senapati, A.K. Singh, T. Arbneshi, S.A. Khan, H.T. Yu, P.C. Ray, ACS Nano 4 (2010) 1739–1749.
[38] X.X. Cao, S.H. Li, L.C. Chen, H.M. Ding, H. Xu, Y.P. Huang, J. Li, N. Liu, W. Cao, Y. Zhu, B. Shen, N. Shao, Nucl. Acids Res. 37 (2009) 4621–4628.
[39] A.H. Hopman, F.C. Ramaekers, E.J. Speel, J. Histochem. Cytochem. 46 (1998) 771–777.
[40] H.J. Qi, S.H. Chen, M.L. Zhang, H. Shi, S.Q. Wang, Anal. Bioanal. Chem. 398 (2010) 2745–2750.
[41] K. Zaitsu, Y. Ohkura, Anal. Biochem. 109 (1980) 109–113.
[42] E.J. Speel, H.N. Anton, J. Histochem. Cytochem. 47 (1999) 281–288.
[43] T.G. Miao, Z.P. Wang, S. Li, X. Wang, Microchim. Acta 172 (2011) 431–437.
[44] V. Escamilla-Gomez, S. Campuzano, M. Pedrero, J.M. Pingarron, Talanta 77 (2008) 876–881.
[45] S. Boujday, R. Briander, M. Salmain, J.M. Herry, P.G. Marnet, M. Gautier, C. M. Pradier, Microchim. Acta 163 (2008) 203–209.
[46] X.H. Xue, J. Pan, H.M. Xie, J.H. Wang, S. Zhang, Talanta 77 (2009) 1808–1813.
[47] G.A. Zelada-Guillen, J.L. Sebastian-Avila, P. Blondeau, J. Riu, F.X. Rius, Biosens. Bioelectron. 31 (2012) 226–232.